Coupling between Catalysis and Oligomeric Structure in Nucleoside Diphosphate Kinase

Sébastien Mesnildrey, Fabrice Agou, Anna Karlsson, Dominique Deville Bonne, Michel Véron

THE JOURNAL OF BIOLOGICAL CHEMISTRY
Vol. 273, No. 8, Issue of February 20, pp. 4436–4442, 1998
Printed in U.S.A.

Coupling between Catalysis and Oligomeric Structure in Nucleoside Diphosphate Kinase*

(Received for publication, October 16, 1997, and in revised form, November 28, 1997)

Sébastien Mesnildrey‡, Fabrice Agou§, Anna Karlsson¶, Dominique Deville Bonne, and Michel Véron‖

From the Unité de Régulation Enzymatique des Activités Cellulaires Institut Pasteur, CNRS URA 1149, 25 rue du Docteur Roux, 75724 Paris, Cedex 15, France

A dimeric *Dictyostelium* nucleoside diphosphate kinase has been stabilized by the double mutation P100S-N150stop which targets residues involved in the trimer interface (Karlsson, A., Mesnildrey, S., Xu, Y., Moréra, S., Janin, J., and Veron, M. (1996) *J. Biol. Chem.* 271, 19928–19934). The reassociation of this dimeric form into a hexamer similar to the wild-type enzyme is induced by the presence of a nucleotide substrate. Equilibrium sedimentation and gel filtration experiments, as well as enzymatic activity measurements, show that reactivation of the enzyme closely parallels its reassociation. A phosphorylatable intermediate with low activity participates in the association pathway while the dimeric form is shown totally devoid of enzymatic activity. Our results support the hypothesis that different oligomeric species of nucleoside diphosphate kinase are involved in different cellular processes where the enzymatic activity is not required.

Nucleoside diphosphate kinase (NDP kinase)[1] is an ubiquitous enzyme involved in the equilibration of NTP cellular pools. It catalyzes the transfer of a phosphate group from a nucleoside triphosphate to a nucleoside diphosphate in the presence of divalent cations, preferably Mg^{2+}. The reaction involves the formation of a covalent intermediate where the enzyme is phosphorylated on the catalytic histidine. NDP kinase has broad specificity and can use indifferently ribo- or deoxyribonucleotides of purines or pyrimidines (1).

Apart from its role in nucleotide metabolism, NDP kinase is reportedly involved in a variety of cellular functions. In human, four NDP kinase genes have been isolated (2–5). The human Nm23-H1 isoform, also called NDPK-A, was isolated as a potential metastasis suppressor (reviewed in Ref. 6). Mutations in *nm23-H1* were shown to lack motility suppressive capacity and were shown associated with histidine-dependent protein phosphotransfer (7). A S120G mutation was found in Nm23-H1 in advanced neuroblastoma (8) that could be related to a defect in protein folding (9). The NDPK-B, encoded by the gene *nm23-H2*, was shown to bind to the nuclease hypersensitive element of the c-*myc* promoter (10) as well as to single strand DNA and RNA sequences (11). This DNA binding activity is maintained in a catalytically inactive mutant (12). In *Escherichia coli*, also, there is indication that NDP kinase may be involved in signal transduction in phosphorylating and activating two different histidine kinases (13). Altogether, these results indicate that NDP kinase is a multifunctional protein that carries other function(s) than its catalytic activity of nucleotide phosphotransfer. The molecular bases of these different functions are poorly understood.

About 50 NDP kinase genes have been cloned, both from eukaryotes and prokaryotes. All NDP kinases are oligomeric proteins made of 17–20-kDa subunits with highly conserved sequences. The crystal structures of several NDP kinases have also been determined, including from the eukaryotes *Dictyostelium discoideum* (14), *Drosophila melanogaster* (15), and human (16, 17), and the prokaryote *Myxococcus xanthus* (18). The secondary structure and the fold of the subunit are highly conserved with the same $\beta\alpha\beta\beta\alpha\beta$ motif found in all structures (19). This homology extends to the association areas of the subunits within dimers, which are almost identical in all NDP kinases (19). However, the oligomeric structures are different. While prokaryotic enzymes were found as tetramers, eukaryotic NDP kinases are hexamers. It is interesting to note that the subunit of prokaryotic enzymes from *M. xanthus* and *E. coli*, which form tetramers, are 5–7 residues shorter at the C terminus than the subunit from eukaryotic NDP kinases.

In the *Dictyostelium* NDP kinase, as in all the hexameric NDP kinases, the dimer interface involves helices α1 and strands β2, which form an intersubunit antiparallel β-sheet between two monomers (14). The trimer interface (Fig. 1) involves three main contacts between subunits: (*a*) hydrogen bonds between Pro-105 and water molecules at the 3-fold axis, (*b*) hydrogen bonds between Pro-100 and residues 110–113 in one subunit and Lys-35 in the other, and (*c*) a hydrogen bond between Asp-115 and the C-terminal Glu-155 of the neighbor subunit (19). Several of the amino acids participating in these contacts are contained in a large loop called the "Kpn loop" (residues 99–119).

Using site-directed mutagenesis we have previously engineered mutant *Dictyostelium* NDP kinases with a disrupted trimer interface. Thus, P105G mutant protein was shown to reversibly dissociate at 2 M urea in contrast to the wild-type protein, which is stable up to 5 M urea (20, 21). The P100S and P100G mutant proteins as well as proteins carrying small deletions at the C terminus (including the N150Stop deleted of

* This work was supported in part by grants from the Association pour la Recherche sur le Cancer and Ligue Contre le Cancer (Comité de Paris). The costs of publication of this article were defrayed in part by the payment of page charges. This article must therefore be hereby marked "*advertisement*" in accordance with 18 U.S.C. Section 1734 solely to indicate this fact.

‡ Supported by a fellowship from the Association pour la Recherche sur le Cancer and the foundation Pasteur-Weissmann.

§ Supported by the Ligue Nationale Contre le Cancer.

¶ Supported by a fellowship from INSERM. Present address: Dept. of Medical Biochemistry and Biophysics, Karolinska Institutet, S-171 77 Stockholm, Sweden.

‖ To whom correspondence should be addressed: Unité de Régulation Enzymatique des Activités Cellulaires, INSTITUT PASTEUR, 25 rue du Dr. Roux, 75724, Paris Cedex 15, France. Tel.: 33-1-45-68-84-03; Fax: 33-1-45-68-83-99; E-mail: mveron@pasteur.fr.

[1] The abbreviations used are: NDP, nucleoside diphosphate; Kpn, Killer of Prune; NDPK-A, human NDP kinase A; NDPK-B, human NDP kinase B; FPLC, fast protein liquid chromatography.

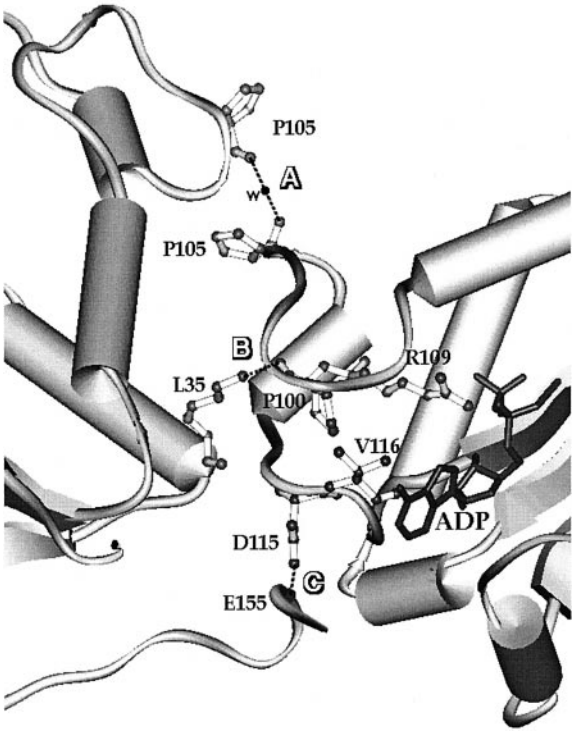

FIG. 1. **The Kpn loop of the *Dictyostelium* NDP kinase.** The Kpn loop containing the amino acids involved in the trimer interface is viewed along the 3-fold axis. It shows the three different contacts between two subunits within a trimer. *A* is made of interactions between Pro-105 of each subunit through a water molecule. *B*, Pro-100 and amino acids 110–113 in one subunit and Lys-35 in the other; *C*, Asp-115 and the C-terminal Glu-155 of the neighbor subunit. Arg-109, Val-116, and Asn-119 participating in the active site are also shown.

the 5 C-terminal amino acids) were also engineered (22). These proteins are synthesized in recombinant bacteria as active hexamers but their stabilities toward temperature and urea denaturation are severely affected. However, the x-ray structures of the P105G (23) and P100S (22) mutant proteins are very similar to that of the wild-type protein.

Pro-100, totally conserved in all NDP kinases, corresponds to contact B in the trimer interface described in Fig. 1. The P100S substitution in *Dictyostelium* NDP kinase, corresponding to the P97S mutation in *Drosophila*, has no effect on the catalytic activity but the protein becomes unstable, presumably due to the dissociation of the hexamer (22, 24). The P97S mutation in *Drosophila* NDP kinase gene corresponds to the *kpn* mutation, which leads to a lethal phenotype in the absence of the *prune* gene product (25). When the P100S mutation and the deletion of the C terminus were combined in the double mutant P100S-N150stop, the recombinant protein was synthesized in bacteria as a stable dimer with a specific activity of less than 1% as compared with the wild-type enzyme (22).

In this paper, we report the study of the oligomerization equilibrium of NDP kinase upon binding of its nucleotide ligands. The possible relevance of changes in the oligomerization state to biological process in the cell is discussed.

MATERIALS AND METHODS

Protein Purification—Wild-type NDP kinase was purified as described (26) with some modifications. *E. coli* XL1-Blue (500 ml) were grown at 37 °C overnight in LB medium containing 200 μg/ml ampicillin and 10 μg/ml tetracycline. After harvest by centrifugation, the cells were resuspended in 50 mM Tris-HCl, pH 8.4, containing 5 mM $MgCl_2$ and broken in a French Press. After centrifugation (50,000 × *g*) for 30 min at 4 °C, the supernatant was loaded on a Q-Sepharose (Pharmacia) column equilibrated with 50 mM Tris-HCl buffer, pH 8.4, containing 0.5 mM EDTA. The recombinant enzyme, recovered in the flow-through fraction, was approximately 70% pure as juged by SDS-polyacrylamide gel electrophoresis and was free from contaminating *E. coli* NDP kinase. The pH was adjusted to 7.4 and NDP kinase was further purified by affinity chromatography on Blue Sepharose (Pharmacia) after elution by a 0–2 M NaCl gradient. Fractions were concentrated and the excess salt removed by ultrafiltration (Amicon). For the P100S-N150stop mutant NDP kinase, the Blue Sepharose column was replaced by a Dye Matrex Orange A column (Amicon). The protein was then eluted by a 0–1 M NaCl gradient and concentrated. The purity of each protein was determined by SDS-polyacrylamide gel electrophoresis. Protein concentration was determined either by the method of Bradford (27) or by absorbance at 280 nm using an extinction coefficient of 0.548 (wild-type) and 0.49 (mutated enzyme) for 1 mg/ml solutions.

NDP Kinase Assay and Reactivation Experiments—In a standard assay, NDP kinase activity was measured at 20 °C by a coupled assay (28) in T buffer (50 mM Tris-HCl, pH 7.5, containing 75 mM KCl and 5 mM $MgCl_2$) supplemented with 1 mg/ml bovine serum albumin, 0.2 mM dTDP, and 1 mM ATP. The kinetic parameters (K_m and k_{cat}) were determined using a constant ratio for the two substrates α = [dTDP]/[ATP] with [ATP] varying from 0.2 to 2 mM. Two values of α were used (0.1 and 0.05). All measurements were made in duplicate or triplicate. For reactivation experiments, P100S-N150stop mutant NDP kinase at the indicated concentration (expressed in subunits) was incubated during various times up to 20 h in presence of 1 mM ATP or ADP in buffer T containing 1 mg/ml bovine serum albumin. NDP kinase (10 to 50 ng/assay) activity was then measured by the coupled assay. When reconstitution of hexameric NDP kinase was analyzed by fluorescence or gel filtration, the experiments were done in the same conditions, but without addition of bovine serum albumin to buffer T.

Steady-state Fluorescence—All fluorescence measurements were performed at 20 °C in buffer T on a PTI spectrofluorometer Quantamaster™. The excitation wavelength was 295 nm to minimize the contribution of tyrosyl residues to the total fluorescence as well as light absorption by ATP. The excitation and emission bandwidths were both set to 2.5 nm. The spectra were corrected by subtracting background intensities of a blank solution made of buffer solution with the added nucleotide. The time course experiments were achieved in the same conditions and the emission of fluorescence was recorded at 340 nm.

Analytical Gel Filtration and Autophosphorylation Assays—FPLC gel filtration of NDP kinase was carried out using a Superose HR 12 10/30 (Pharmacia) column equilibrated in buffer T′ (50 mM Tris-HCl, pH 7.5, containing 150 mM KCl and 5 mM $MgCl_2$) and developed at a flow rate of 0.3 ml/min. In some experiments, the elution buffer was buffer T′ containing 500 μM ATP.

For the autophosphorylation assays, NDP kinase (15 μM) was incubated during 1 min, 3 h, or 24 h with various concentrations of [γ-^{32}P]ATP (0–2 mM) in buffer T′ in a total volume of 100 μl. [γ-^{32}P]ATP (4,500 Ci/mmol) was from ICN. The total radioactivity used for each assay was 1.5 μCi. The components of the mixture were then separated on FPLC. The elution of the protein was monitored by absorbance at 220 nm and the radioactivity was counted in each fraction (fraction volume = 0.3 ml). The stoichiometry of the phosphorylated enzyme was determined from the ratio of radioactive phosphate incorporated to the concentration of protein in subunits.

Analytical Ultracentrifugation—Sedimentation equilibrium experiments were performed at 20 °C in a Beckman Optima XL-A analytical ultracentrifuge, using an An-60 Ti rotor and a double-sector cell of 12-mm path length. Enzyme samples were dialyzed exhaustively against three changes of buffer T′ alone or buffer T′ containing ATP (500 μM). The reference cells were filled by the buffer used for the last dialysis. Enzyme was allowed to reach equilibrium at three speeds in a single run (9,000, 12,000, and 18,000 rpm). Equilibrium was verified from the superimposition of duplicate scans recorded at 2-h intervals. The experimental data were first fitted to a model for a single homogeneous species following the equation (29),

$$c_{(r)} = c_{(\mathrm{ref})}\exp\{[(M(1 - v\rho)\omega^2/2RT](r^2 - r^2_{\mathrm{ref}})\} + \delta \qquad \text{(Eq. 1)}$$

$c_{(r)}$ is the concentration of the protein at radial position r, $c_{(\mathrm{ref})}$ is the concentration of the protein at an arbitrary reference distance r_{ref}, M is the molecular weight, mdity the partial specific volume of the solute, ρ is the density of the solvent, ω is the angular velocity, R and T are the molar gas constant and the absolute temperature, respectively, and δ is the base line offset. The partial specific volume was calculated from the amino acid composition of the protein sample, and the density of the buffers was determined from published tables (29). When the experimentally determined value of M did not converge on the true mass of the single homogeneous species (16,168 Da for monomer or n × 16,168

Da for n-mer), the data were fitted to a n-mer-i-mer equilibrium, according to Equation 2, where $c_{\text{i-nmer}}$ are the concentrations of the i-nmer,

$$c(r) = \sum_{i} c_{\text{i-nmer}}(r_{\text{ref}})\exp\{[(\text{in M}(1 - v\rho)\omega^2/2RT](r^2 - r_{\text{ref}}^2)\} + \delta \quad \text{(Eq. 2)}$$

In all cases, since inclusion of a second virial coefficient gave no improvement of the fit, an ideal component system was considered. The data were fitted to the models with the Levenberg-Marquardt algorithm in the commercially available graphics software package KaleidaGraph.

RESULTS

The P100S-N150stop Dimeric NDP Kinase Is Catalytically Inactive—The mutant P100S-N150stop NDP kinase displays an absorbance spectrum similar to that of the wild-type enzyme in its folded conformation (not shown). The single tryptophan residue present in wild-type NDP kinase is conserved in the mutant protein and was used to study the protein fluorescence. Upon denaturation, the intrinsic fluorescence is strongly quenched and the maximum wavelength of the spectrum is shifted from 335 to 350–355 nm (30). The emission fluorescence spectrum of dimeric NDP kinase upon excitation at 295 nm is also very similar to the wild-type spectrum whether in its folded conformation or unfolded in 10 M urea (not shown). This indicates that the enzyme subunits are folded with similar conformations in the dimeric and in the wild-type hexamer.

The combination of the P100S mutation with deletion of the five C-terminal residues results in an enzyme with very little activity: Table I shows a comparison of the kinetic parameters of the double mutant P100S-N150stop with those of the wild-type NDP kinase. The K_M^{ATP} and K_M^{dTDP} are similar. In contrast, the k_{cat} value for the mutant protein was about 5% of that of the wild-type enzyme, a value in agreement with our previous measure of the specific activity (22).

TABLE I
Kinetic parameters of P100S-N150stop NDP kinase

Enzymatic activity was determined using 65 μM protein (subunits) by the coupled assay at 20 °C. k_{cat} values are calculated per active site.

Specific activity	Wild type NDP kinase	P100S-N150stop NDP kinase	Reactivated P100S-N150stop NDP kinase
units/mg			
	2200 ± 200	100 ± 20	2200 ± 200
k_{cat} (s^{-1})	620 ± 50	27 ± 5	600 ± 50
K_M^{ATP} (mM)	0.3 ± 0.1	0.5 ± 0.1	0.2 ± 0.1
K_M^{dTDP} (mM)	0.08 ± 0.02	0.05 ± 0.01	0.1 ± 0.01

However, in contrast to the wild-type enzyme, we observed that the enzymatic activity of the P100S-N150stop NDP kinase varies with protein concentration. While in the condition of the experiment shown in Table I (1.1 mg/ml, *i.e.* 64 μM subunits) the residual activity was 5% of wild type, it was less than 0.05% when the enzyme solution was diluted to 1 μM for 24 h (not shown). The decrease in specific activity was slow and only appeared several hours after the dilution of the enzyme. Since the K_m values for both substrates are similar to that of the wild-type enzyme, the above observation indicated that the residual activity of the P100S-N150stop NDP kinase may be due to the presence of a small amount of hexamers, rather than to an intrinsic residual activity of the dimer.

Reactivation and Reassociation of the P100S-N150stop NDP Kinase in the Presence of Nucleotides—The addition of substrates to the dimeric mutant protein was found to affect its enzymatic activity. Fig. 2 shows the time-dependent increase in NDP kinase activity upon addition of 1 mM ATP to the P100S-N150stop mutant protein. After 3 h incubation in the presence of 30 μM subunits, the activity recovered was similar to that of the wild-type enzyme (about 2,000 units/mg). The fact that the reactivation is complete indicates that no irreversible aggregation occurred during the 3 h of incubation (31). The time course of the reactivation is described by a second-order reaction without any lag, indicating that the limiting step is a bimolecular process (Fig. 2, *inset*). A second-order rate constant of 10^4 $M^{-1} \times s^{-1}$ was calculated from the double reciprocal plot of the data collected at two protein concentrations. A similar reactivation was found after overnight incubation of the dimeric NDP kinase in the presence of GTP (results not shown). The reactivation of P100S-N150stop NDP kinase could also be induced by 500 μM ADP with a similar time course (Fig. 2), indicating that

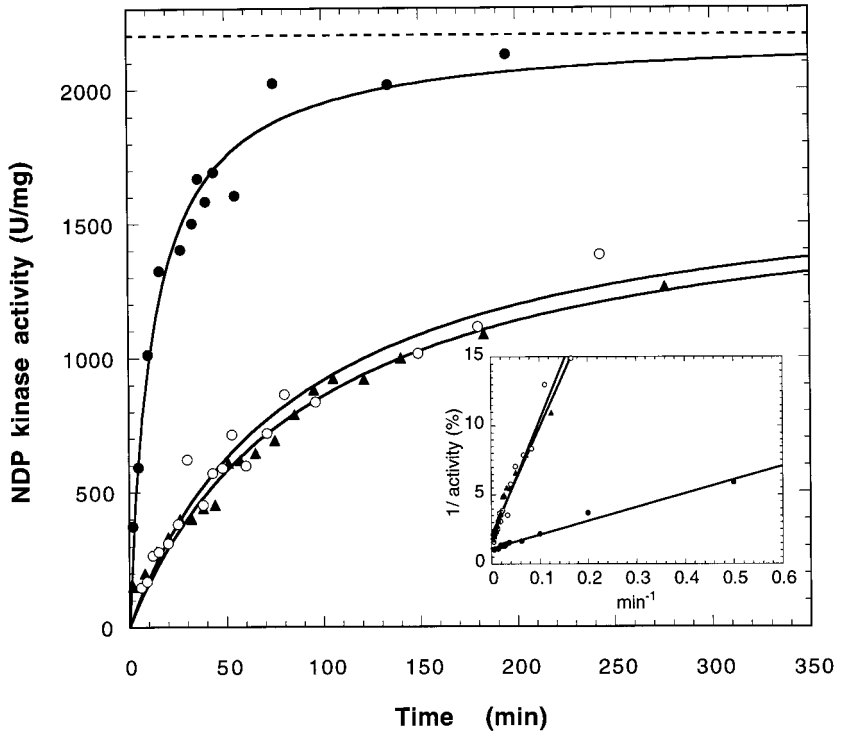

FIG. 2. **Reactivation of the P100S-N150stop protein.** P100S-N150stop NDP kinase was incubated in buffer T′ at two concentrations in the presence of 500 μM ATP at 20 °C and the increase in activity upon time was measured using the coupled assay (6.5 μM NDP kinase subunits (○); 30 μM (●)). A similar experiment with 6 μM P100S-150stop protein in the presence of 500 μM ADP is also shown (▲). *Inset*, second-order double-reciprocal plot of the kinetics of reactivation of NDP kinase. The observed rate constants are 1.1×10^4 $M^{-1} \cdot s^{-1}$ and 0.95×10^4 $M^{-1} \cdot s^{-1}$, respectively, for 30 and 6.5 μM NDP kinase reactivated in the presence of ATP.

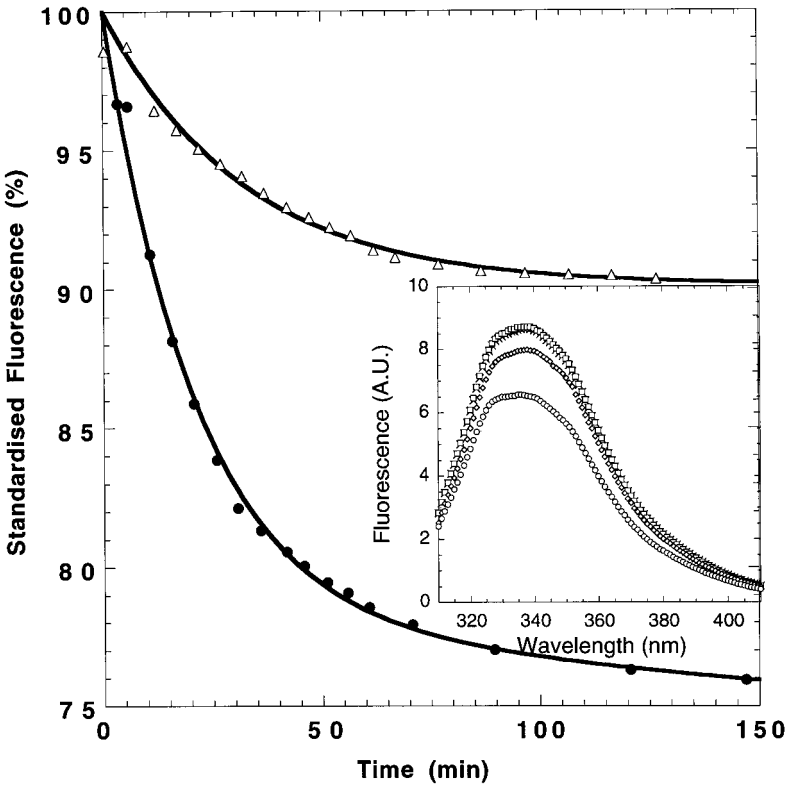

FIG. 3. **Kinetics of reactivation of the P100S-N150stop protein monitored by fluorescence.** The fluorescence of the protein was measured in buffer T as a function of time after addition of 500 μM ATP (●) or ADP (△). The *inset* represents the fluorescence emission spectra of the P100S-N150stop protein in the presence of ATP or ADP. The protein was incubated in buffer T with saturating amounts of nucleotides during 1 min or 3 h: □, no addition; ×, after 1 min in the presence of 500 μM ATP; ○, after 3 h in the presence of 500 μM ATP; ⋆, after 3 h in the presence of 500 μM ADP.

the phosphorylation of the catalytic histidine is not necessary to the reactivation process.

As shown in Fig. 3, the fluorescence properties of P100S-150stop enzyme change upon nucleotide addition. The *inset* in Fig. 3 shows that the intrinsic fluorescence of the dimeric enzyme is insensitive to ADP or ATP when it is measured immediately after nucleotide addition. In contrast, the fluorescence level decreases by 25% upon preincubation with ATP and by 10% upon ADP incubation. This signal was used to monitor the kinetics of the structural transition of dimeric NDP kinase upon nucleotide addition (Fig. 3).

We then performed sedimentation equilibrium measurements of P100S-N150stop NDP kinase before and after ATP-induced reactivation of the enzyme in the presence or absence of 500 μM ATP at a single initial loading concentration and at three different rotor speeds (Fig. 4 and Table II). In the absence of ATP, the molecular mass deduced from the fit is 34,000 ± 2,000 Da in accordance with the theoretical mass of 2 × 16,168 Da for a dimer. At 18,000 rpm, some hexamer (5%) could also be detected at the bottom of the cell, where the enzyme concentration is high. When the centrifugation was performed with the reactivated P100S-N150stop enzyme in the presence of ATP, we used two wavelengths, 280 and 295 nm, to determine the relative concentration of the ATP bound to the enzyme. In the presence of 500 μM ATP, the ATP-bound enzyme fraction was 98%, indicating that all sites of the enzyme were saturated. The distribution of P100S-N150stop NDP kinase, obtained for three rotor speeds, could be fitted to a single homogeneous species with a molecular mass corresponding to a hexamer (6 × 16,168 Da). We conclude that upon incubation with saturating amounts of ATP or ADP, the P100S-N150stop mutant protein recovers all of the functional properties of the native NDP kinase due to the reassociation of the dimers into hexamers.

The Dimeric NDP Kinase Is Unable to Autophosphorylate—Although the residual activity of the P100S-N150stop NDP kinase appears to be carried by the hexamer as shown above, the dimeric form may still catalyze the phosphotransfer even at a lower rate. The enzyme should then be fully phosphorylated on the catalytic histidine upon addition of ATP. We analyzed the content of phosphorylated protein after a short pulse of [γ-^{32}P]ATP to prevent dimer reassociation. For this, the double mutant enzyme (15 μM) was incubated during 1 min with [γ-^{32}P]ATP in low amount (25 μM), and the mixture was analyzed by FPLC on a Superose 12 column. The dimeric form was separated from hexameric form and [γ-^{32}P]ATP. As shown in Fig. 5, the protein eluted in three peaks. Peak H, corresponding to the hexamer (elution volume, 11.6 ml), was sparsely populated. Most of the protein was found at the elution volume of the dimer (peak D) (13.5 ml). An unexpected third component (peak I) was also observed. [^{32}P] radioactivity was associated with peaks H and I but was totally absent from peak D, demonstrating that the dimeric NDP kinase is not able to autophosphorylate.

An Intermediate in ATP-induced Reassociation of Dimeric NDP Kinase—Fig. 6 shows an analysis of the reassociation reaction of the P100S-N150stop protein in the presence of increasing concentrations of ATP. The elution profile from the Superose column indicates that the hexameric wild-type enzyme is homogeneous, as shown by the occurrence of a single peak (elution volume 11.3 ml) (Fig. 6*a*). The peak corresponding to the dimer in the absence of ligands (elution volume 13.5 ml) (Fig. 6*b*) is slightly asymmetric, possibly indicating some dissociation into monomers. When ATP is added to the dimeric enzyme, the elution profile is strongly affected (Fig. 6, *c-f*). The proportion of dimeric enzyme (*D*) decreases in the presence of increasing amounts of ATP, and a new species (*I*), with an elution volume of 12.9 ml, appears. At higher ATP concentration, the hexameric species (*H*) is also present. The fact that the increase in [ATP] does not change the position of the peaks in the elution diagram indicates a slow interconversion between species D, I, and H. Fig. 7 shows a representation of the fraction of NDP kinase present as species D, I, and H after 1 min at different ATP concentrations. There is an excellent correlation between the disappearance of D and the formation of I and H.

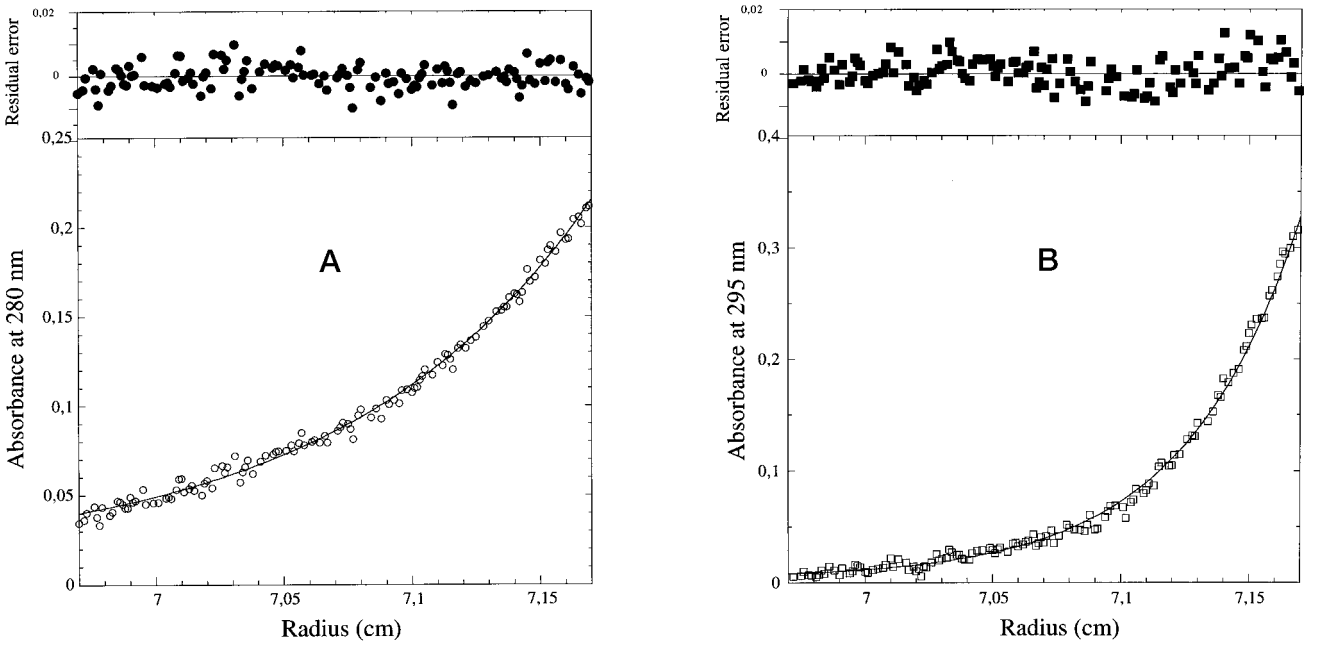

FIG. 4. **Sedimentation equilibrium distribution of P100S-N150stop NDP kinase.** The relative concentration of P100S-N150stop NDP kinase in the absence (*A*) or presence of ATP (500 μM) (*B*), measured by its absorbance at 295 nm, was plotted as a function of the radial distance at 18,000 rpm. The experimental data (*open circles* and *squares*) were fitted (*curves*) as described under "Materials and Methods." Residuals (indicated above each fit) were obtained from the best global fit of the experimental data to the dimer-hexamer model (*A*) or to a single homogeneous species model (*B*).

TABLE II
Summary of sedimentation equilibrium experiments with P100S-N150stop NDP kinase

In all experiments, the concentration of protein loaded in the centrifuge cells at the beginning of the experiment was 40 μM.

ATP	Angular velocity	Wavelength	M_r[a]	χ^{2a}	$\chi^2_{\alpha_2 \rightarrow \alpha_6}$[b]	Distribution of molecular species
μM	*rpm*	*nm*	*Da*			%
0	9,000	280	34,000 ± 2,000	90		100 α_2
0	12,000	280	33,000 ± 1,500	80		100 α_2
0	18,000	280	35,000 ± 3,000	150	88	95 α_2, 5 α_6
500	9,000	280, 295	97,000 ± 1,800	70		100 α_6
500	12,000	280, 295	96,000 ± 2,000	72		100 α_6
500	18,000	280, 295	95,000 ± 2,000	100		100 α_6

[a] The weight-average molecular mass is calculated by fitting the equilibrium sedimentation data to a single ideal species as described under Materials and Methods.

[b] Value is obtained for bispecies model dimer-hexamer. χ^2 is the weighted sum of squared residuals and gives criteria for the quality of the fit.

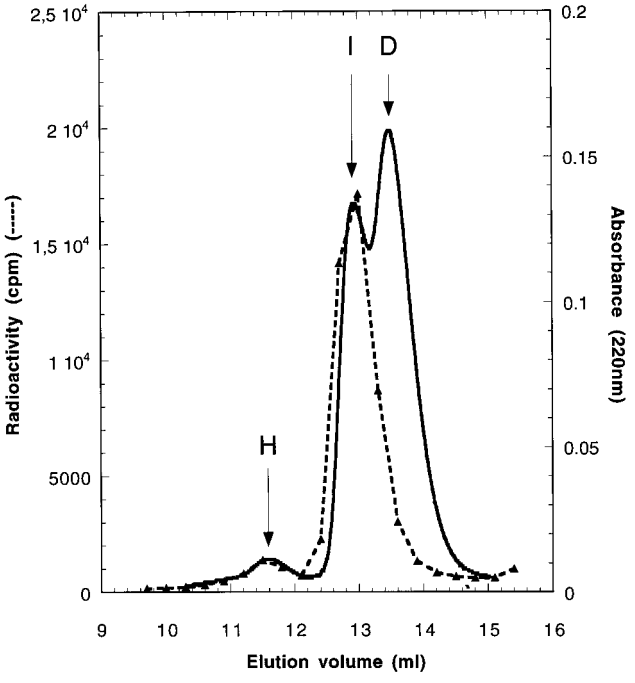

FIG. 5. **Autophosphorylation followed by gel filtration.** 15 μM P100S-N150stop protein was incubated for 1 min in presence of [γ-^{32}P]ATP (50 μM) in a final volume of 100 μl and loaded on a FPLC Superose 12 column (Pharmacia). The elution of the protein was followed by absorbance at 220 nm (*black line*) and by radioactive counting of the fractions (0.3 ml) (*dotted line*). *H*, *I*, and *D* indicate the elution position of, respectively, the hexamer, of the intermediate and dimer.

The disappearance of I and the formation of H are also correlated for the higher ATP concentrations. Thus, I appears to be an intermediate in the reassociation process. After 3 h in the presence of 0.5 mM ATP, the elution profile is similar to Fig. 6*f* (result not shown). No radioactivity was ever associated with component D. In contrast, components I and H were phosphorylated with a stoichiometry of 1 phosphate per subunit.

DISCUSSION

We have demonstrated that the dimeric P100S-N150stop mutant NDP kinase is able to reassociate into a hexameric enzyme and that recovery of enzymatic activity closely parallels reassociation. Both the dimeric and the hexameric species involved in this equilibrium are precisely defined. The P100S-N150stop mutant NDP kinase purified from recombinant bacteria is a well folded dimeric protein as shown by its fluorescence spectrum and equilibrium sedimentation. The reassociated enzyme obtained in the presence of substrate is hexameric as demonstrated by equilibrium ultracentrifugation and has the same turnover and substrate specificity as the wild-type enzyme. The transition from the dimer to the hexamer is concentration and time dependent. It is induced both by ADP and ATP, indicating that binding of the nucleotide is important rather than the phosphorylation of the catalytic histidine. No aggregate could be detected during the reassociation process in agreement with previous urea denaturation-

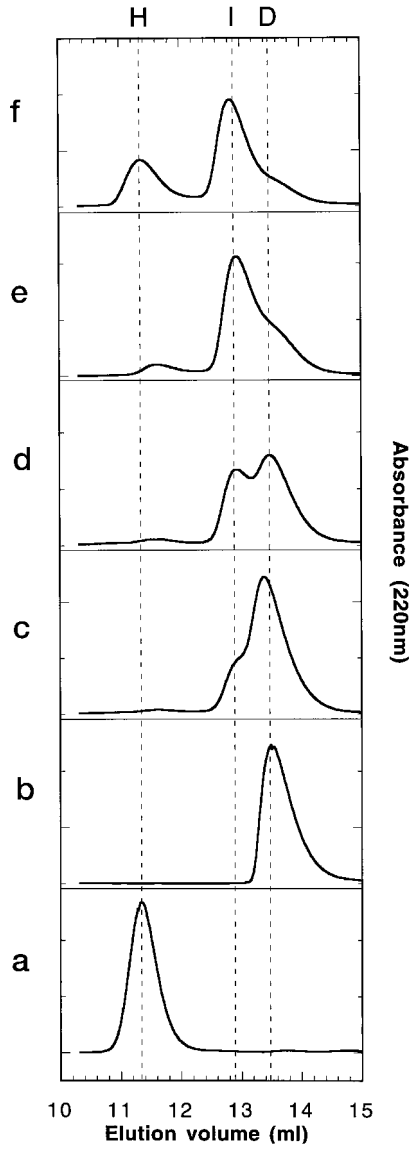

FIG. 6. **Reassociation of the P100S-N150stop upon incubation with ATP followed by gel filtration.** The protein (15 μM) was incubated for 1 min with various concentrations of ATP in a final volume of 100 μl and loaded on the FPLC Superose 12 column. The elution of the protein was monitored by absorbance at 220 nm. *a*, wild-type enzyme; *b-f*, P100S-N150stop kinase (15 μM) in the absence (*b*) or presence of ATP: 25 μM (*c*), 50 μM (*d*), 500 μM (*e*), and 2 mM ATP (*f*).

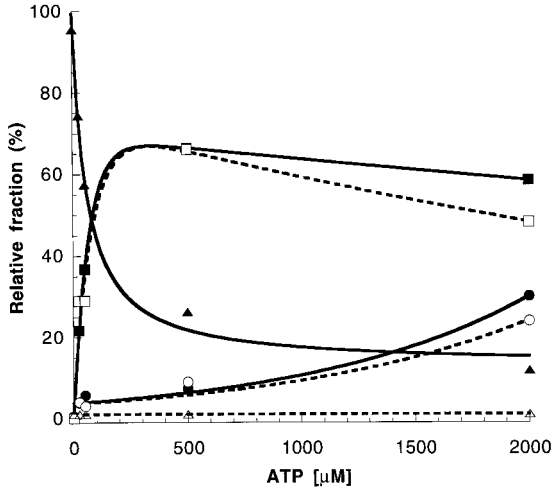

FIG. 7. **Changes in the oligomeric state of P100S-N150stop NDP kinase.** The relative fraction of the different oligomeric state in experiments shown in Fig. 6 was derived from the peak areas of the elution profile: dimer (▲), intermediate (■), and hexamer (●). The incorporated radioactive phosphate (—-) was determined from the radioactivity measured in a given fraction and expressed relative to the total radioactivity incorporated: dimer (Δ), intermediate (□), and hexamer (○).

renaturation experiments using the wild-type and the Pro-105 mutant NDP kinase (21). The recovery of the fluorescence sensitivity to nucleotides in the reassociated hexamer can be explained either by local or indirect structural changes around the single Trp-137. In both cases, it indicates a structural change within the dimers upon assembly into hexamers. Although the reassociated enzyme solution has the maximal specific activity found for the wild-type NDP kinase (2000 units/mg), and its equilibrium sedimentation and fluorescence properties are identical to the native hexameric enzyme, the conversion of the dimer into hexamer is only partial when analyzed by FPLC (Fig. 6). This discrepancy is probably due to some dissociation of the reconstituted hexamer during the course of the FPLC column.

The kinetic data of the reassociation obtained at two different protein concentrations indicate that the reaction is second-order rather than third-order as would be expected for the reassociation of three dimers into a single hexamer (see Fig. 2). In agreement with a bimolecular reactivation process, a possible reassembly scheme could involve two consecutive reactions with the formation of an intermediate. In such an assembly pathway, the first step is likely the association of two dimers into a tetrameric intermediate, while the second reaction, a rate-limiting bimolecular process, would restore the enzymatic activity upon association of the intermediate with another dimer. In agreement with this scheme, an intermediate is indeed observed on the oligomerization pathway (Fig. 5). We estimated directly its relative amount by measuring the area of the corresponding peak after elution from FPLC. The size of this new species is intermediate between that of the dimer and the hexamer, as estimated from its elution volume. This intermediate appears very rapidly. After 1 min in the presence of 0.5 mM ATP, it represents more than 60% of the enzyme molecules (Fig. 6*e*). However, the enzymatic activity is still low at this time, representing only 5% of the fully active enzyme (Fig. 2), strongly indicating that the specific activity of the intermediate is very low, although it is fully autophosphorylated (Fig. 5). These two observations are not contradictory: indeed, it should be noted that a low specific activity (*e.g.* 0.1% of wild-type) still results in the full phosphorylation of the catalytic histidine within less than 1 s, due to the high turnover of the enzyme.

The surprising unability of the dimeric P100S-N150stop mutant NDP kinase to autophosphorylate on the catalytic histidine (Figs. 5 and 6) suggests that the dissociated enzyme is not able to bind properly the nucleotide substrate. We propose that the dimeric NDP kinase is in equilibrium between two conformations differing in their ability to bind a nucleotide, according to Scheme 1,

$$D' \rightleftarrows D \rightleftarrows I \rightleftarrows H$$

SCHEME 1

where D (dimer), I (intermediate), and H (hexamer) bind ADP or ATP with a good affinity. The states D and I (possibly a tetramer) are competent for assembly while D′ does not bind nucleotides. At low concentration of protein and in the absence of nucleotide, the enzyme is likely to be in equilibrium between D and D′ with little [D]. ATP addition displaces this toward D, which rapidly associates in I and then more slowly into H. At

high protein concentrations, the enzyme should be essentially under the H state.

The close relationship between the ability of the dimeric mutant protein to bind the nucleotide and its ability to assemble into hexamers can be explained by some particular features of the NDP kinase subunit structure. Each nucleotide-binding site is only made of residues of one subunit. It involves residues belonging to the central β sheet and to the so-called Kpn loop (residues 99–119). The latter include Val-116, Asn-119, and Arg-109 contributing to the binding, respectively, of the base, the ribose, and the phosphate moieties of the nucleotide (32). Considering that all the contacts of the trimer interface (noted *A, B,* and *C* in Fig. 1) require amino acids of the Kpn loop, the correlation between the nucleotide-binding site and assembly competence is likely to reside in the conformation of the Kpn loop. In the hexamer, the three Kpn loops come together at the center of one trimer. We propose that the formation of the trimeric interface induces the productive conformation of the nucleotide-binding site and reciprocally, that the binding of a nucleotide results in the restructuration of the Kpn loop so that stronger contacts within the interface can occur. In the P100S-N150stop mutant protein, the disruption of contacts B and C is likely to result in an improper conformation of the Kpn loop and an impaired binding of the nucleotide. Previous studies on NDP kinase mutated at Pro-105 (contact A) also reported an effect of ADP on subunit assembly during renaturation after urea treatment (21, 23). It thus appears that disruption of the trimer interface in contacts A, B, or C produces analogous structural changes for the enzyme.

The question then arises whether the assembly pathway of the P100S-N150stop mutant NDP kinase described here is a model for both the wild-type *Dictyostelium* enzyme and for NDP kinases from other eukaryotes and whether there is a specific functional role for the different oligomeric forms of the protein. It is tempting to speculate that either the dimeric form of the enzyme and/or the intermediate could play a specific role in function(s) of NDP kinase not directly related to its catalytic activity to phosphorylate nucleosides diphosphate. First, the intermediate, which is able to autophosphorylate, could be involved in the phosphorylation of non-nucleotidic substrates due to an increased flexibility of its active site that could accommodate bulkier substrates. Thus, in the case of the *Killer of prune* (*Kpn*) mutant *Drosophila*, the lethal phenotype may be due to the ability of the mutant NDP kinase to phosphorylate an unknown compound that would specifically accumulate in the absence of the *prune* gene product and have toxic effects (33). NDP kinase has also recently been shown to phosphorylate proteins in the presence of small amounts of urea (34) and the phospho-transfer from the catalytic histidine of human NDP kinase A to aspartate or glutamate residues of a 43-kDa protein was tentatively correlated with the suppression of tumor metastasis of some cell lines (35). The inspection of the crystal structure of hexameric NDP kinases makes unlikely the transfer from the active site phosphohistidine to protein substrates unless a major conformational change occurs. The intermediate in the oligomeric assembly described in this paper could provide a structural basis for the putative protein kinase activity of NDP kinase.

A role for the oligomeric state of NDP kinase in its DNA binding activity is also emerging from recent studies. The DNA binding activity of human NDPK-B does not require its catalytic activity (12) and the amino acids involved in this process are localized near the symmetry axis of the dimer (36). Recently, an *in vitro* study showed an increased affinity of DNA oligonucleotides for the P100S-N150Stop mutant NDP kinase from *Dictyostelium*, as compared with the wild-type hexameric enzyme (37). Future work is needed to determine the oligomeric state of the protein binding to DNA *in vivo* and to unravel the mechanism(s) by which it is controlled in the cell.

Acknowledgments—We thank Professors Joël Janin for stimulating discussions and Manuel Babolat for performing NDP kinase autophosphorylation assays.

REFERENCES

1. Parks, R. E. J., and Agarwal, R. P. (1973) *The Enzymes* **8,** 307–334
2. Steeg, P. S., Bevilacqua, G., Kopper, L., Thorgeirsson, U. P., Talmadge, J. E., Liotta, L. A., and Sobel, M. E. (1988) *J. Nat. Cancer Inst.* **80,** 200–204
3. Stahl, J. A., Leone, A., Rosengard, A. M., Porter, L., King, C. R., and Steeg, P. S. (1991) *Cancer Res.* **51,** 445–449
4. Venturelli, D., Martinez, R., Melotti, P., Casella, I., Peschle, C., Cucco, C., Spampinato, G., Darzynkiewicz, Z., and Calabretta, B. (1995) *Proc. Natl. Acad. Sci. U. S. A.* **92,** 7435–7439
5. Milon, L., Rousseau-Merck, M., Munier, A., Erent, M., Lascu, I., Capeau, J., and Lacombe, M. (1997) *Hum. Genet.* **99,** 550–557
6. De La Rosa, A., Williams, R. L., and Steeg, P. S. (1995) *BioEssays* **17,** 53–62
7. Freije, J. M. P., Blay, P., MacDonald, N. J., Manrow, R. E., and Steeg, P. S. (1997) *J. Biol. Chem.* **272,** 5525–5532
8. Chang, C. L., Zhu, X. X., Thoraval, D. H., Ungar, D., Rawwas, J., Hora, N., Strahler, J. R., Hanash, S. M., and Radany, E. (1994) *Nature* **370,** 335–336
9. Lascu, I., Schaertl, S., Wang, C., Sarger, C., Giartosio, A., Briand, G., Lacombe, M. L., and Konrad, M. (1997) *J. Biol. Chem.* **272,** 15599–15602
10. Postel, E. H., Berberich, S. J., Flint, S. J., and Ferrone, C. A. (1993) *Science* **261,** 478–480
11. Hildebrandt, M., Lacombe, M.-L., Mesnildrey, S., and Veron, M. (1995) *Nucleic Acids Res.* **23,** 3858–3864
12. Postel, E. H., and Ferrone, C. A. (1994) *J. Biol. Chem.* **269,** 8627–8630
13. Lu, Q., Park, H., Egger, L. A., and Inouye, M. (1996) *J. Biol. Chem.* **271,** 32886–32893
14. Dumas, C., Lascu, I., Morera, S., Glaser, P., Fourme, R., Wallet, V., Lacombe, M.-L., Veron, M., and Janin, J. (1992) *EMBO J.* **11,** 3203–3208
15. Chiadmi, M., Moréra, S., Lascu, I., Dumas, C., LeBras, G., Veron, M., and Janin, J. (1993) *Structure* **1,** 283–293
16. Morera, S., Lacombe, M.-L., Xu, Y., LeBras, G., and Janin, J. (1995) *Structure* **3,** 1307–1314
17. Webb, P. A., Perisic, O., Mendola, C. E., Backer, J. M., and Williams, R. L. (1995) *J. Mol. Biol.* **251,** 574–587
18. Williams, R. L., Oren, D. A., Munoz-Dorado, J., Inouye, S., Inouye, M., and Arnold, E. (1993) *J. Mol. Biol.* **234,** 1230–1247
19. Morera, S., Dumas, C., Lascu, I., Lacombe, M.-L., Veron, M., and Janin, J. (1994) *J. Mol. Biol.* **243,** 373–390
20. Lascu, I., Deville-Bonne, D., Glaser, P., and Veron, M. (1993) *J. Biol. Chem.* **268,** 20268–20275
21. Lascu, I., Deville-Bonne, D., Glaser, P., and Veron, M. (1994) *J. Biol. Chem.* **269,** 7046; Correction (1993) *J. Biol. Chem.* **268,** 20268–20275
22. Karlsson, A., Mesnildrey, S., Xu, Y., Morera, S., Janin, J., and Veron, M. (1996) *J. Biol. Chem.* **271,** 19928–19934
23. Giartosio, A., Erent, M., Cervoni, L., Morera, S., Janin, J., Konrad, M., and Lascu, I. (1996) *J. Biol. Chem.* **271,** 17845–17851
24. Lascu, I., Chaffotte, A., Limbourg-Bouchon, B., and Veron, M. (1992) *J. Biol. Chem.* **267,** 12775–12781
25. Sturtevant, A. H. (1956) *Genetics* **41,** 118–123
26. Tepper, A., Dammann, H., Bominaar, A. A., and Veron, M. (1994) *J. Biol. Chem.* **269,** 32175–32180
27. Bradford, M. M. (1976) *Anal. Biochem.* **72,** 248–254
28. Segel, I. H. (1975) in *Enzyme Kinetics*, 1993 Ed., pp. 608–612, John Wiley & Sons, Inc., New York
29. Laue, T. M., Bhaivari, D. S., Ridgeway, T. M., and Pelletier, S. L. (1992) in *Analytical Ultracentrifugation in Biochemistry and Polymer Science* (Harding, S. E., Rowe, A. J., and Horton, J. C., eds) pp. 90–125, Royal Society of Chemistry Press, Cambridge, United Kingdom
30. Deville-Bonne, D., Sellam, O., Merola, F., Lascu, I., Desmadril, M., and Veron, M. (1996) *Biochemistry* **35,** 14643–14650
31. Jaenicke, R., and Rudolph, R. (1986) *Methods Enzymol.* **131,** 218–250
32. Morera, S., Lascu, I., Dumas, C., LeBras, G., Briozzo, P., Veron, M., and Janin, J. (1994) *Biochemistry* **33,** 459–467
33. Timmons, L., and Shearn, A. (1997) *Adv. Genet.* **35,** 207–252
34. Engel, M., Veron, M., Theisinger, B., Lacombe, M.-L., Seib, T., Dooley, S., and Welter, C. (1996) *Eur. J. Biochem.* **234,** 200–207
35. Wagner, P., Steeg, P., and Vu, N. (1997) *Proc. Natl. Acad. Sci. U. S. A.* **94,** 9000–9005
36. Postel, E. H., Weiss, V. H., Beneken, J., and Kirtane, A. (1996) *Proc. Natl. Acad. Sci. U. S. A.* **93,** 6892–6897
37. Mesnildrey, S., Agou, F., and Veron, M. (1997) *FEBS Lett.* **48,** 53–57